Astronomy
&
Astrophysics

The hard X-ray view of the low-luminosity blazar in the radio galaxy NGC 6251

M. Guainazzi[1], P. Grandi[2], A. Comastri[3], and G. Matt[4]

[1] XMM-Newton Science Operations Center, VILSPA, ESA, Apartado 50727, 28080 Madrid, Spain
   e-mail: mguainaz@xmm.vilspa.esa.es
[2] Istituto di Astrofisica Spaziale e Fisica Cosmica (IASF-C.N.R.), Sezione di Bologna, via Gobetti 101, 40129 Bologna, Italy
[3] I.N.A.F., Osservatorio Astronomico di Bologna, via Ranzani 1, 40127 Bologna, Italy
[4] Dipartimento di Fisica, Università degli Studi "Roma Tre", via della Vasca Navale 84, 00146 Roma, Italy

Abstract. We present results from a BeppoSAX (July 2001) observation of the FR I radio galaxy NGC 6251, together with a re-analysis of archival ASCA (October 1994) and *Chandra* (September 2000) data. The weak detection above 10 keV and the lack of iron fluorescent K_α emission lines in the BeppoSAX spectrum rule out that the bulk of the X-ray emission is due to an obscured Seyfert nucleus. The study of the multiwavelength spectral energy distribution suggests instead that X-rays probably originate as inverse-Compton of synchrotron seed photons in a relativistic jet, indicating that NGC 6251 hosts a low radio luminosity ($L_{5\ \mathrm{GHz}} \sim 10^{40}$ erg s^{-1}) blazar. The BeppoSAX spectrum is flatter than in the earlier ASCA observation. This might be due to the emergence of a different spectral component during phases of lower X-ray flux. In this context, we discuss some possible explanations for the intense and mildly-ionized fluorescent iron line measured by ASCA.

1. Introduction

NGC 6251 is an E2 nearby ($z = 0.02488$; if $H_0 = 70$ km s^{-1} Mpc^{-1}, as assumed in this paper, 1″ corresponds to about 500 pc) radio galaxy with a Faranoff-Riley I morphology, known to host a giant radio jet (Wagget et al. 1977), a Seyfert 2 nucleus (Werner et al. 2002), and almost edge-on dust lanes (Nieto et al. 1983). The nucleus is likely to contain a supermassive black hole with mass $M \sim 4$–$8 \times 10^8\ M_\odot$ (Ferrarese & Ford 1999), as suggested by the presence of nuclear gas and a dust disc on scales of a few hundreds parsecs. NGC 6251 belongs to the outskirts of the cluster Zw 1609.0+8212 (Young et al. 1979), whose influence on the properties of the galaxy should be, however, marginal (Prestage & Peacock 1988).

The NGC 6251 jet is one of the most spectacular radio objects of the whole sky. It is a 4′.5 long, highly collimated (opening angle 7.4°) structure (Perley et al. 1984). Regions of enhanced radio emission along the jet were labeled by Birkinshaw & Worrall (1993) in the 330 MHz radio map as A (10–40″ from the nucleus), B (40–126″; actually structured in smaller sub-structures) and D (178–264″, where the jet bends towards the North; it is as well highly structured). Between B and D one finds a region of low radio brightness (C). None of these region was observed to be a significant source of X-ray emission by ROSAT (Birkinshaw & Worrall 1993). A sub-pc

counter-jet was discovered only recently with Very Long Baseline Interferomer observations (Sudou et al. 2001). *U*-band *Hubble Space Telescope* images unveiled a region of extended emission, lying nearly perpendicular to the radio jet axis and the dust ring (Crane & Vernet 1997), which is likely to originate from scattering of a nuclear continuum source.

Discovered in the X-rays by the *Einstein* Imaging Proportional Counter (Jones et al. 1986), NGC 6251 showed in the ROSAT PSPC observation (Birkinshaw & Worrall 1993) an unresolved core ($FWHM < 4″$), with a possible extended halo on scales $\lesssim 100$ kpc (Mack et al. 1997). The first observation of NGC 6251 covering the intermediate X-rays (i.e.: 2–10 keV) was performed by ASCA. The presence of a bright K_α fluorescence iron from ionized iron (centroid energy, $E_c \simeq 6.68$ keV; Equivalent Width, $EW \simeq 600$ eV; Turner et al. 1997a; Sambruna et al. 1999), and the fact that the continuum could be best fit with a combination of a standard AGN power-law component (photon index, Γ, of 2.11) plus a thermal soft excess, suggested that ionized gas may significantly contribute in this energy band. Electron scattering of an otherwise invisible nuclear continuum was an interesting possibility, in light of the HST discovery of extended ionized gas, which could potentially act as a nuclear mirror ("warm mirror" hereinafter). Recently, an association has been proposed between NGC 6251 and the EGRET source 1EGJ 1621+8203 (Mukherjee et al. 2002). If this is confirmed, NGC 6251 would be one of the three radio galaxies – alongside with Cen A (Sreekumar et al. 1999) and 3EG J1735–1500

(Combi et al. 2003) – detected in high-energy γ-rays. No detection by the *Extreme Ultraviolet Explorer* is reported in the literature (Marshall et al. 1995).

The deep BeppoSAX observation, described in this paper, aimed at verifying the interpretation scenario emerging from the ASCA outcomes. Thanks to its unsurpassed sensitivity in hard X-rays (i.e.: >10 keV; Boella et al. 1997), BeppoSAX would be easily able to detect a transmitted nuclear component piercing through a Compton-thick absorber (Matt et al. 2000). The results of this observation are presented in this paper, together with an analysis of archival ASCA and *Chandra* data of the same source. The log of the observations discussed in this paper is presented in Table 1.

While this paper was in the process of being accepted, we became aware of a recently accepted paper by Chiaberge et al. (2003), who discuss the same X-ray observations, together with literature and HST data. Their X-ray results are largely coincident with ours.

2. BeppoSAX results

2.1. Data reduction

BeppoSAX data were reduced according to standard procedures as in, e.g., Guainazzi et al. (1999). Scientific products for the imaging Low Energy Concentrator Spectrometer (LECS, Parmar et al. 1997, 0.5–4 keV) and Medium Energy Concentrator Spectrometer (MECS, Boella et al. 1997b, 1.8–10.5 keV) were extracted from circular regions of 8′ and 4′, respectively. Background spectra were extracted from blank sky field event lists provided by the BeppoSAX Science Data Center, and appropriate for the date of the observation. Products for the Phoswitch Detector System (PDS, Frontera et al. 1997, 13–200 keV) were extracted by plain subtraction of those corresponding to intervals when the instrument was observing NGC 6251, and a region ±3.5° aside, according to the standard 96 s cycle.

All the spectra employed in this paper have been rebinned in order to oversample the intrinsic energy resolution of the instruments by a factor not larger than 3, and to have a number of counts in each spectral channel higher than 30, in order to ensure the applicability of the χ^2 test. In this paper: energies are quoted in the source rest frame; uncertainties on the spectral parameters are quoted at the 90% confidence level for one interesting parameter; uncertainties on the count rates are at 1σ level, unless otherwise specified.

2.2. Spectral results

In Fig. 1 the results of the fit of the NGC 6251 BeppoSAX spectrum with a simple absorbed power-law is shown. The fit is statistically acceptable (χ^2 = 96.7/92 degrees of freedom, d.o.f.). The best-fit parameters and results are reported in Table 2. The PDS data points lay actually above the best-fit model, which is mainly determined by the statistics of the imaging instruments. The excess is, however, not highly significant. The ratio between the PDS flux and the extrapolation of the best fit model in the LECS/MECS energy band is 1.4 ± 0.6,
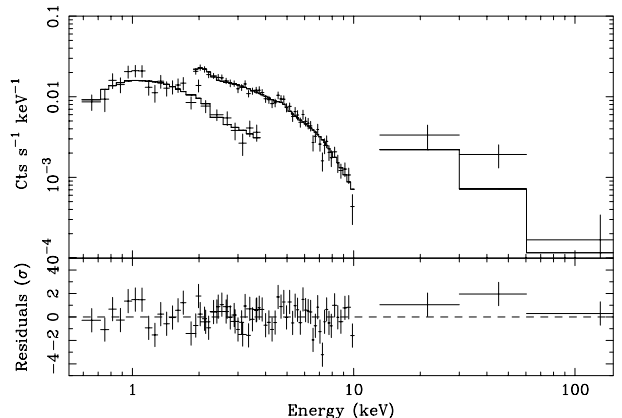

Fig. 1. BeppoSAX spectrum (*upper panel*) and residuals in units of standard deviations (*lower panel*), when the a photoelectrically absorbed power-law model is applied.

therefore only marginally exceeding the typical values of the cross-normalization factors between the PDS and the MECS (0.80–0.85; Fiore et al. 1998). Not surprisingly, several models provide comparably good descriptions of this hard excess, but none of them is required from the statistical point of view. A broken power-law, for instance, yields a $\Delta\chi^2$ = 3.4 for a reduction of the number of degrees of freedom ($\Delta\nu$) by 2 (this quantity will be indicated as $\Delta\chi^2/\Delta\nu$ hereinafter), corresponding to a confidence level $\simeq$83.0%

The BeppoSAX large source spectrum extraction region encompasses the putative ROSAT extended emission. We therefore tried to add a soft X-ray component, modeled by a collisionally ionized plasma (we used the mekal implementation in XSPEC v11.0 throughout this paper; Mewe et al. 1985; Liedahl et al. 1995; Arnaud & Raymond 1992). Again, the improvement in the quality of the fit is not significant ($\Delta\chi^2/\Delta\nu$ = 4.4/2). Consequently, the temperature is rather poorly determined ($kT = 1.4^{+0.9}_{-0.7}$). The 0.5–2.4 keV flux of this component would be $(1.3 \pm 0.7) \times 10^{-13}$ erg cm^{-2} s^{-1}, corresponding to about 15% of the non-thermal component in the same energy band. This model requires an absorbing column density slightly in excess with respect to the Galactic contribution along the line-of-sight to NGC 6251 (5.7×10^{20} cm^{-2}, Murphy et al. 1996).

No systematic residual feature is present at the energies, where K_α fluorescence transitions of iron are expected. Negligible improvements of the χ^2 are yielded by the addition of a narrow (i.e., intrinsic width, σ = 0) Gaussian profile to the power-law model. 90% upper limits on the intensity of a neutral (6.4 keV) or He-like (6.7 keV) iron lines are 8.5 and 3.0×10^{-6} photons cm^{-2} s^{-1}, respectively, corresponding to *EW*s of 160 and 60 eV, respectively. These upper limits are largely inconsistent with the ASCA detection (Turner et al. 1997a; cf. also Sect. 3.1 later). Simulations show that a 600 eV *EW* line would have been detected at the 6–7σ confidence level in the MECS spectrum.

The 0.5–10 keV flux during the BeppoSAX observation was 7.5×10^{-12} erg cm^{-2} s^{-1}, corresponding to un unabsorbed rest-frame luminosity of 1.13×10^{43} erg s^{-1} in the same energy band.

Table 1. Log of the observations presented in this paper.

Satellite	Start time	Exposure time	Count rate
		(ks)	$(10^{-2}$ s$^{-1})$
ASCA	28-Oct.-1994	$36^a/44^b$	$7.2 \pm 0.2^a/3.63 \pm 0.13^b$
Chandra/ACIS-I	11-Sep.-2000	25	8.1 ± 0.2
BeppoSAX	19-Jul.-2001	$28^c/80^d/72^e$	$2.78 \pm 0.12^c/5.55 \pm 0.09^d/13 \pm 4^e$

[a] SIS0, [b] GIS2, [c] LECS, [d] MECS, [e] PDS.

Table 2. Best-fit parameters and results for the analysis of the nuclear spectra of NGC 6251. Model legenda: PL = power-law; TH = thermal component (`mekal` implementation in XSPEC) with solar abundances; GA = Gaussian emission line; BKPL = broken power-law.

Model	$N_{\rm H}$	Γ	$kT_1/\Gamma_{\rm soft}$	$kT_2/E_{\rm break}$	$E_{\rm c}$	$I_{\rm c}$	EW	χ^2/ d.o.f.
Mission	$(10^{21}$ cm$^{-2})$		(keV)/	(keV)	(keV)	$(10^{-6}$ ph cm^{-2} s$^{-1})$	(eV)	
BeppoSAX								
PL	$0.8\pm^{0.6}_{0.3}$	$1.79\pm^{0.06}_{0.07}$	...	...	...	...	...	96.7/92
PL+TH	$1.0\pm^{0.12}_{0.05}$	$1.70\pm^{0.12}_{0.16}$	$1.4\pm^{0.9}_{0.7}$	...	$6.4^\dagger$	<8.0	<160	92.3/90
				...	$6.59^\dagger$	<4.5	<80	
				...	$6.7^\dagger$	<3.0	<60	
				...	$6.96^\dagger$	<2.1	<50	
ASCA								
PL	$0.9\pm^{0.4}_{0.3}$	$2.06\pm^{0.08}_{0.07}$	...	...	...	...	...	259.7/225
PL+TH	$1.6\pm^{0.7}_{0.8}$	$2.00\pm^{0.08}_{0.07}$	$0.85\pm^{0.34}_{0.15}$	...	...	...	...	240.6/223
PL+2×TH	$1.6\pm^{2.1}_{0.8}$	2.3 ± 0.4	$0.8\pm^{0.3}_{0.2}$	$6\pm^6_2$	...	...	...	231.8/221
PL+TH+GA	$1.7\pm^{0.5}_{0.4}$	$2.05\pm^{0.11}_{0.10}$	$0.84\pm^{0.27}_{0.18}$		6.59 ± 0.16	8 ± 4	500 ± 200	228.1/221
BKPL+GA	$4.0\pm^{1.8}_{1.5}$	$2.28\pm^{0.17}_{0.14}$	$3.7\pm^{1.2}_{0.9}$	$1.38\pm^{0.15}_{0.09}$	$6.62\pm^{0.12}_{0.18}$	10 ± 4	800 ± 300	245.0/226

[†] Gaussian emission profiles added to the best-fit continuum. Centroid energies $E_{\rm c}$ are fixed. Upper limits are at the 90% confidence level.

3. Comparison with previous X-ray observations

3.1. ASCA

We have retrieved the data of the ASCA observation of NGC 6251 from the public archive as screened event lists. Spectra were extracted from regions of radii 4′, 3′.1 and 3′.75 in the SIS0, SIS1 (grade 0, 2, 3, 4) and GIS detectors, respectively (they therefore encompass as well the ROSAT extended emission region). Background spectra were extracted from regions in the field of view of the detectors, free from contaminating sources. Response matrices were generated with the packages included in the LHEASOFT v5.0 software. The spectral analysis was performed in the 0.5–10 keV and 0.7–10 keV energy bands, for the SIS and GIS instruments, respectively. The results of our analysis substantially coincide with those presented by Turner et al. (1997) and Sambruna et al. (1999), and we summarize them in this paper for the sake of clarity only.

A simple power-law is a fairly good representation of the ASCA spectra ($\chi^2 = 259.7/225$ d.o.f.). However, the addition of a `mekal` component improves significantly the quality of the fit ($\Delta\chi^2/\Delta\nu = 19.1/2$, corresponding to an F-test confidence level $\simeq$99.97%). The addition of a multitemperature blackbody (model `diskbb` in XSPEC) yields, on the contrary, a negligible improvement to the quality of the fit. Modeling the continuum in terms of a broken power-law yields a comparatively worse fit as well. A systematic excess around the energy where fluorescent K_α transitions from iron are expected
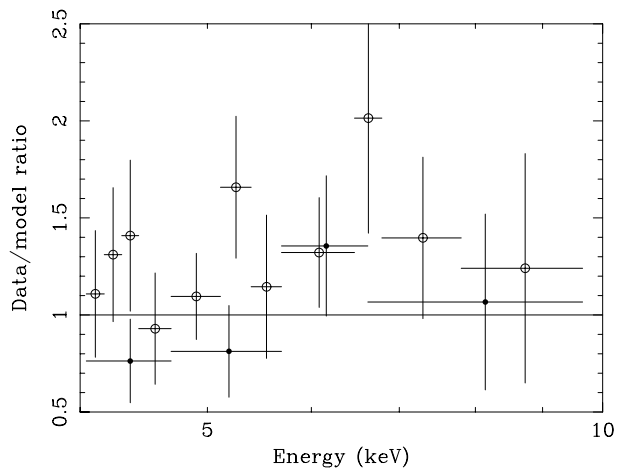

Fig. 2. GIS2 (*filled dots*) and GIS3 (*open circles*) residuals against a power-law plus optically thin thermal plasma continuum in the 4–10 keV bands.

is observed (see Fig. 2). It can be cured with an unresolved Gaussian profile ($\Delta\chi^2/\Delta\nu = 12.5/2$, corresponding to a confidence level $\simeq$99.7%), or with a hotter ($kT \simeq 6$ keV) thermal component ($\Delta\chi^2/\Delta\nu = 8.8/2$, corresponding to a confidence level $\simeq$98.6%).

In the best-fit model (cf. Table 2), the power-law index ($\Gamma \simeq 2.05$) is significantly steeper than observed by BeppoSAX. The temperature of the colder thermal component is $kT \simeq 0.8$ keV, and its 0.5–2.4 keV flux (($1.6 \pm 0.4) \times 10^{-13}$ erg cm^{-2} s^{-1}) is

in good agreement with that of the corresponding component in the BeppoSAX spectrum. The iron line centroid energy is consistent with K_α fluorescence from mildly ionized to He-like iron. Its EW is 500 ± 200 eV, significantly larger than the upper limits measured by BeppoSAX. The difference is most likely due to a change in the underlying continuum, as the intensity of the ASCA line (($8 \pm 4) \times 10^{-6}$ photons cm^{-2} s^{-1}) is marginally consistent with the BeppoSAX upper limits. However, an intrinsic variability of the iron line cannot be ruled out.

The observed 0.5–10 keV flux during the ASCA observation was 2.7×10^{-12} erg cm^{-2} s^{-1}, corresponding to an unabsorbed total luminosity of 4.4×10^{42} erg s^{-1} in the same energy band.

3.2. Chandra

Data of an ACIS-I NGC 6251 *Chandra* observation were retrieved from the public archive. A bright source (count rate $(8.1 \pm 0.2) \times 10^{-2}$ s^{-1}) is detected with coordinates: $\alpha_{2000} = 16^h32^m31^s8$; $\delta_{2000} = +82^h32^m16^s$, i.e. 0.6″ distant from the optical nucleus of NGC 6251, well within the accuracy of the *Chandra* attitude reconstruction. At this count rate level, a *Chandra* source is likely to be substantially affected by pile-up, given the instrumental mode employed (Time Exposure Mode with a 3.2 s frame time). We have tried to fit the 0.5–8 keV spectrum extracted from the innermost 5″ with a photoelectrically absorbed power-law, corrected for pile-up according to the XSPEC implementation of J. Davis' algorithm (model `pileup` in XSPEC; Arnaud & Dorman 2002). The fit is acceptable ($\chi^2 = 57.1/78$ d.o.f.), and yields best-fit parameters which are consistent with those measured during the BeppoSAX observation, save a 60% lower flux: $N_H = (1.6 \pm 0.5) \times 10^{21}$ cm^{-2}; $\Gamma = 1.76 \pm 0.16$; 0.5–10 keV flux of 4.5×10^{-12} erg cm^{-2} s^{-1}.

Thanks to the unprecedented spatial resolution of the ACIS-S, the issue of the spatial extension can be better addressed. No evidence for extended emission along the arcminutes scale jet is detected, as the ROSAT observation had already shown in the soft X-rays only (Birkinshaw & Worrall 1993). The upper limits on the X-ray fluxes of the regions A to D are reported in Table 3. They are by a factor 5 to 10 tighter than those determined by Birkinshaw & Worrall (1993). However, the upper limit on the knot "D" flux density is inconsistent with the detection ($S_\nu = 13 \pm 2$ nJy) obtained by Mack et al. (1997) from a reanalysis of the same ROSAT/PSPC observation discussed by Birkinshaw & Worrall (1993).

In the innermost 4′ around the NGC 6251 core only two sources, alongside with the nucleus itself, are detected at a signal-to-noise ratio higher than 3. Their positions and count rates are reported in Table 4. None of them exhibits a clear association with any radio structures.

4. Discussion

4.1. The nature of the nuclear X-ray emission in NGC 6251

The main goal of the BeppoSAX observation described in this paper was to test whether the strong ($EW \sim 600$ eV),
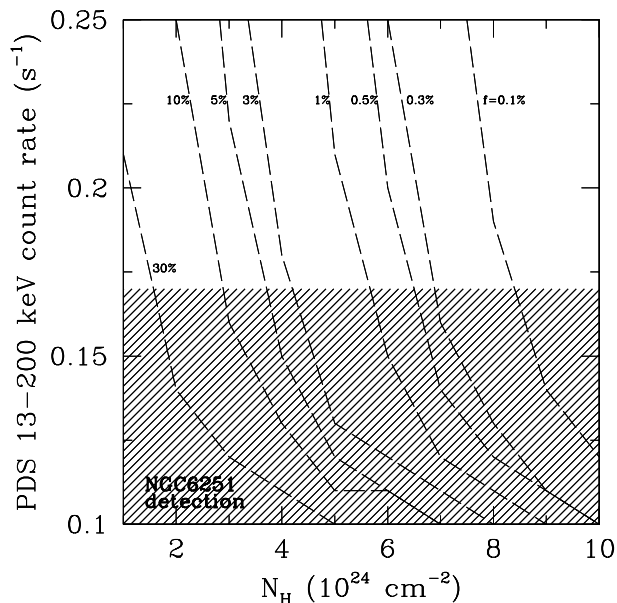

Fig. 3. PDS count rates in the 13–200 keV energy band against the column density of a Compton-thick absorber covering the NGC 6251 nucleus, for different values of the scattering fraction f. The *shaded area* indicates the PDS detection yielded by the BeppoSAX observation of NGC 6251. f is defined by the ratio between the normalizations of the transmitted and the warm scattered components, assuming an optically thin scatterer.

ionized K_α fluorescent iron line observed in the ASCA spectrum (Turner et al. 1997a) was due to a "warm mirror" reflection-dominated, Compton-thick Seyfert 2 spectrum. In the light of the BeppoSAX observation outcomes, this possibility is rather unlikely. The PDS detection (0.13 ± 0.04 s^{-1} in the 13–200 keV energy band) is statistically consistent with the extrapolation of the 2–10 keV spectrum. This constraints the column density of any Compton-thick absorber to the nucleus to be $\gtrsim 3 \times 10^{24}$ (6×10^{24}) cm^{-2} for a 10% (1%) scattering fraction (see Fig. 3). Moreover, the 2–10 keV BeppoSAX spectrum lacks any trace of fluorescence K_α ionized iron lines, which are almost always observed in reflection-dominated Seyfert 2 galaxies (Turner et al. 1997b; Matt et al. 2000). The upper limits on their EWs are rather strict, ranging between 60 and 80 eV for He- and H-like iron. The standard AGN 2–10 keV spectral index ($\Gamma \simeq 1.7$), and the lack of K_α neutral iron line (again, with a rather tight EW upper limit: 160 eV) in the BeppoSAX spectrum rule out a significant contribution by Compton-reflection from the inner side of the molecular torus (Krolik et al. 1994; Ghisellini et al. 1994; Matt et al. 1996) In principle, the line flux could be suppressed by resonant trapping at the ionized surface of an accretion disk (Matt et al. 1993). However, further pieces of evidence rule out that the X-ray spectrum is dominated by reflection of an otherwise invisible Seyfert nucleus.

Some hints come from the study of the multiwavelength Spectral Energy Distribution (SED). Recently, Fossati et al. (1998) have proposed a unified scheme to explain the multiwavelenght SED of blazars, whose properties (peak frequency of the synchrotron and inverse-Compton components,

Table 3. 90% upper limits on the ACIS-I count rates (CR), 0.5–10 fluxes (F), and 1 keV flux density (S_ν) across the NGC 6251 jet regions (following their definition in Birkinshaw & Worrall 1993). The distance d is defined from the inner-outer border of each region to the core. Fluxes are calculated assuming a power-law spectrum, with $\Gamma = 2$ and photoelectric absorption column density $N_H = 5.7 \times 10^{20}$ cm^{-2}.

Region	d	Area	CR	F	S_ν
	(arcsec)	(arcsec^2)	(10^{-4})	[a]	(nJy)
A	10–40	46.8	2.8	2.3	0.34
B	40–126	140.6	2.2	1.8	0.26
C	126–178	78.1	2.9	2.4	0.36
D	178–264	124.9	1.9	1.6	0.24

[a] In the 0.5–10 keV band, in units of 10^{-15} erg cm^{-2} s^{-1}.

Table 4. Sources detected in the ACIS-I observation of the NGC 6251 field, within 4′ from the core.

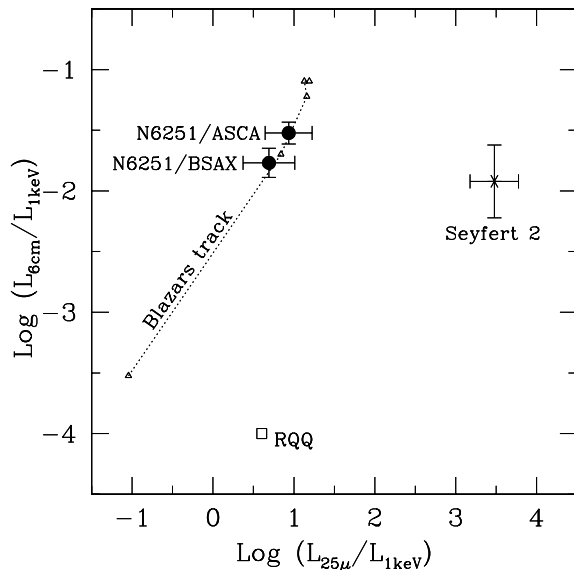| #	α_{2000}	δ_{2000}	count rate
			(10^{-4} s^{-1})
1	$16^h32^m31^s.8$	$+82^h32^m16^s$	810 ± 20[a]
2	$16^h33^m00^s.5$	$+82^h31^m12^s$	4.8 ± 1.8
3	$16^h33^m21^s.3$	$+82^h31^m56^s$	5.6 ± 1.8

[a] NGC 6251 nucleus.

Fig. 4. Radio (6 cm), X-ray (0.5–4.5 keV) and IR (25 μ) color-color diagram. The *dotted line* represents the blazar track according to the blazar unified scheme of Fossati et al. (1998). The *filled circles* represent the data points corresponding to the NGC 6251 ASCA and BeppoSAX observations. The *cross* corresponds to the Seyfert 2 sample of Mass-Hesse et al. (1995). The *empty square* represents the SED of radio-quiet quasars (Elvis et al. 1994).

luminosity ratio between them) are mainly governed by a single parameter related to the overall luminosity. This scheme can be applied to help identifying the nature of the bulk of the X-ray emission from the NGC 6251 nucleus. In Fig. 4 we show a color-color diagram between the radio ($\nu = 6$ cm), soft X-ray (0.5–4.5 keV), and infrared ($\lambda = 25\ \mu$) luminosities. The dotted line in this diagram represents the trace followed by blazars according to the Fossati scheme. In the same plot the cross represents the position of the Seyfert 2 galaxies of the Mass-Hesse et al. sample (1995). The 6 cm radio luminosity of NGC 6251 is $(1.0 \pm 0.1) \times 10^{40}$ erg s^{-1} (Jones et al. 1986). The data points corresponding to the ASCA and BeppoSAX observations lay intriguingly well on the blazar track. This supports the idea that the bulk of the nuclear emission in NGC 6251 is due to a jet.

Chiaberge et al. (1999) discovered a clear correlation between the optical (F_O) and the radio core luminosity (F_R) in a sample of FRI galaxies extracted from the 3C catalogue and observed with the HST WFC2. Assuming the NGC 6251 SED published by Ho (1999), $\log(F_R/F_O) \simeq 3.4$, in perfect agreement with the value derived from the 3C correlation (3.7 ± 0.4; the uncertainties represent the rms scattering of the data points in the correlation), and largely inconsistent with values typically measured in radio-loud quasars ($\simeq -1$; Elvis et al. 1994). This supports a common origin for the radio and optical emission as synchrotron radiation. HST observations in the U-band measured a rather high degree of polarization (close to 50%) in clumps close to the nucleus along the radio axis. Crane & Vernet (1997) suggest that the UV emission of these clumps is due to scattering. However, such an evidence is consistent as well with the possibility that the synchrotron-dominance extends well within the UV range.

We tried to fit the overall NGC 6251 SED from radio to γ-rays (X-rays represented by the BeppoSAX spectrum)

with an homogeneous Synchrotron Self-Compton (SSC) model (Tavecchio et al. 1998). This model assumes that synchrotron radiation is produced by relativistic electrons with density n_e continuously injected in a spherical region of radius r with a magnetic field B and moving with bulk factor Γ_{bulk} at an angle θ with respect to the line of sight (the Doppler factor is therefore $\delta = [\Gamma_{bulk}(1 - \beta\cos\theta)]^{-1}$). These photons are subsequently upscattered by the same electrons. Following Tavecchio et al. (1998), the electron energy distribution is modeled with a broken power-law with indices $n_1 < 3$ and $n_2 > 3$ below and above a break energy γ_b, respectively. The IRAS data points, although in principle available, have not been included in the fit due to the unknown contamination from the host galaxy. The best fit from radio to γ frequencies (*dashed line* in Fig. 5) fails to reproduce the BeppoSAX spectral shape and slightly deviates below 10^{10} Hz. If one forces the model to match the BeppoSAX data point (*dotted line* in Fig. 5), the radio emission is more overproduced. This may indicate that self-absorption (which is not explicitly included in SSC models) plays an important role redwards the synchrotron peak. Given the fact that the SED data points correspond to non-simultaneous observations, one cannot push too far the comparison between the model and the observation. Nonetheless, the overall properties of the best-fit SSC models are not strongly dependent on the details of the fit. The synchrotron peak is below 10^{14} Hz, whereas the Compton peak remains constrained between $10^{21.5}$ and $10^{22.5}$ Hz. As a reference the best-fit parameters for the fits are in the range: $B = 0.01$–0.15 G, $\delta = 2$–4, $n_1 = 1.75$–2.6, $n_2 = 4.1$–5.4, $\gamma_b = 6.3 \times 10^3$–$1.6 \times 10^4$ $n_e = 10^5$–10^6 cm^{-3}, and $r = 1$–8×10^{16} cm. The reader is referred to Chiaberge et al. (2003)
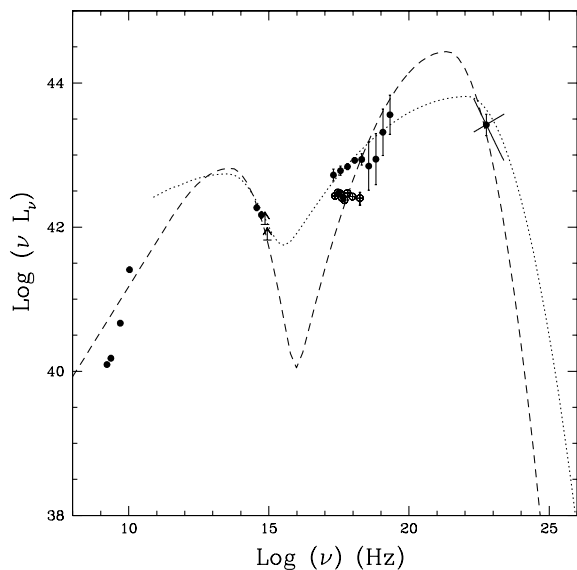
Fig. 5. NGC 6251 SED. Data are from not-simultaneous observations compiled by Ho (1999), save the and X-ray data (BeppoSAX, *dots*; this paper), and the putative EGRET detection. The *dashed line* represents the best radio-γ fit SSC model; the *dotted line* represents the fit with an SSC model, forced to reproduce the BeppoSAX spectral shape. The ASCA spectrum (*empty circles*) is shown as well for reference.

Fig. 6. Radio between the 1 keV and the *V*-band flux density in: **a)** NGC 6251 (*filled circle*); **b)** the blazar radio luminosity classes in the unified scenario after Fossati et al. (1998); **c)** ADAF models applied to a sample of nearby elliptical galaxies (Di Matteo et al. 2000; details in text). In the last case, the error bars on the *y*-axis represent the rms of the sample values in the corresponding radio luminosity interval.

for a more detailed comparison between the NGC 6251 SED and SSC models.

It is hard to interpret the spectral variability between the ASCA (*empty circles* in Fig. 5) and the BeppoSAX spectra in terms of pure SSC model. In principle, the ASCA spectrum may represent the trailing edge of the synchrotron component. However, this would imply a shift of the synchrotron peak by more than 4 orders of magnitude, which is rather unlikely. Alternatively, the steeper ASCA spectrum may imply that a different spectral component may be emerging during phases of low X-ray flux. This component may be completely outshined during BeppoSAX-like, X-ray brighter states. We will further discuss this possibility in Sect. 4.2, in connection with the strong fluorescent iron line observed in the ASCA spectra only.

Recently, it has been suggested that the bulk of the X-ray emission in radio galaxies may be due to a hot inner accretion flow, following a line of thought suggested more than 20 years ago by Rees et al. (1982). Ho (1999) estimates the bolometric luminosity of NGC 6251 as $\sim 10^{-4}\ L_{\mathrm{Edd}}$. This may indicate that an Advection Dominated Accretion Flow (ADAF; Narayan & Yi 1995) is responsible for the bulk of the emission in the NGC 6251 core. In this scenario, X-rays are mainly produced via bremsstrahlung by a distribution of thermal electrons with typical temperatures $kT \sim 100$ keV (Di Matteo et al. 2000). In Fig. 6 we compare the ratio between the *V* and the 1 keV flux density (BeppoSAX measurement) in NGC 6251 with the values expected by the blazar unification scenario (Fossati et al. 1998) and by models of ADAF applied to the multiwavelength SED of nearby elliptical galaxies suspected to host low radiative efficiency accretion flows (Di Matteo et al. 2000; we consider hereby models
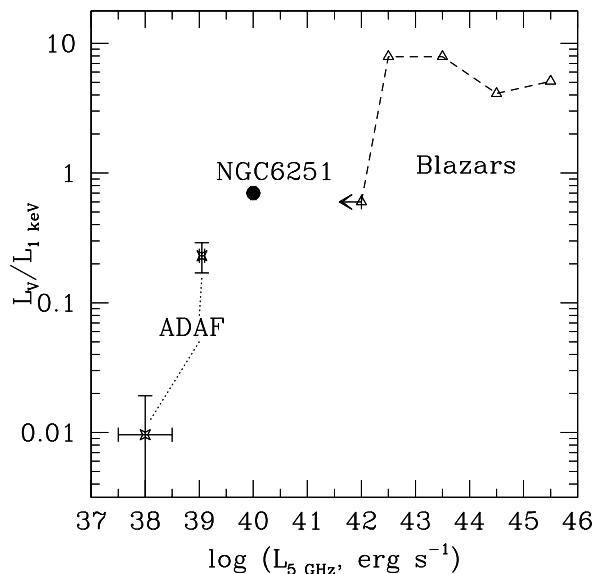
with wind, and outermost hot accretion radius of 300 gravitational radii). The NGC 6251 data point is in principle consistent with both scenarios. Applying a bremsstrahlung model to the BeppoSAX spectrum, one gets indeed a total X-ray luminosity $L_X/L_{\mathrm{Edd}} = (2 \pm 1) \times 10^{-3}$. However, the fit is significantly worse than with a simple power-law ($\chi^2 = 110.0/92$ d.o.f.). A composite bremsstrahlung and power-law fit (the latter component taking into account possible Comptonization effects) yields an implausibly low electron temperature ($kT \simeq 3$ keV). These pieces of evidence are in agreement with the conclusions drawn by Ferrarese & Ford (1999), who remark that the *nuclear* non-thermal bolometric optical luminosity in NGC 6251 is larger than predicted for accretion at the Bondi rate with 10% efficiency, making the case for an ADAF far less compelling.

4.2. Additional components in the nuclear X-ray spectrum of NGC 6251

As already noticed by Turner et al. (1997), a soft X-ray excess is observed in the NGC 6251 ASCA spectra. A multitemperature blackbody is not able to fit the excess, arguing against the possibility that this component originates in an accretion disk. The best-fit temperature of the soft excess, if modeled with an optically thin, collisionally excited plasma, is $kT \simeq 0.8$ keV, with an unabsorbed luminosity of $\simeq 3.6 \times 10^{41}$ erg s^{-1}. Such a temperature is typical of gaseous halos in elliptical galaxies (Matsumoto et al. 1997). The parameters of this component are consistent with those of a similar component in the BeppoSAX spectrum, which is, however, not required from the statistical point of view. The ASCA temperature is in turn consistent, within the rather large statistical uncertainties, with the temperature of the extended halos measured by the

Einstein/IPC and the ROSAT/PSPC in NGC 6251 (for the latter, $kT = 0.3$–0.8 keV; Birkinshaw & Worrall 1993 and references therein). Similarly, the 0.5–2.4 keV unabsorbed fluxes of this component measured by ASCA and BeppoSAX are consistent with the ROSAT/PSPC soft X-ray "halo" flux, integrated across its whole extension (($2.4\pm^{4.2}_{2.0}$) $\times 10^{-13}$ erg cm^{-2} s^{-1}; Mack et al. 1997). It is therefore straightforward to identify the soft excess in the large ASCA aperture with the diffuse emission in ROSAT. Mack et al. (1997) discuss (and rule out) the possibility that such a plasma could be the confining medium for the jet, along the whole structure up to knot "D". A $\simeq 10^7$ K thermal emission responsible for the confinement of the jet in NGC 6251 should not extend beyond scales larger than 60 pc. On such small scales, it might be marginally resolvable by *Chandra*. Unfortunately, the pile-up affecting the *Chandra* observation prevented us from deriving precious constraints on the X-ray extension around the NGC 6251 core.

The ASCA spectrum unveils the possible presence of a third spectral component, whose main signature is a bright ($EW \simeq 600$) eV and significantly ionized K$_\alpha$ fluorescence iron line. This component, even if present with comparable flux in the BeppoSAX observation, would have easily missed detection, due to the fact that the BeppoSAX non-thermal continuum 6 keV flux density was ≥ 6 times larger than in ASCA. This "third" component cannot be produced by the superposition of unresolved discrete sources, integrated in the large ASCA aperture. The *Chandra* image shows only two sources in the innermost 4′ around the NGC 6251 core, whose total count rate [$(1.1 \pm 0.3) \times 10^{-3}$], corresponds to a 0.5–9 keV flux $\simeq 1.0 \times 10^{-14}$ erg cm^{-2} s^{-1} (assuming a thermal plasma with $kT = 6$ keV). This is more than one order of magnitude less than the flux of the ASCA component in the same energy band (2×10^{-13} erg cm^{-2} s^{-1}). This component may therefore represent the "tip of the iceberg" of an underlying Seyfert nuclear "warm scattering" (Matt et al. 1996, 2001), whose relative contribution becomes not-negligible during phases of lower blazar activity. Alternatively, this component may represent a hotter and weaker phase of the thermal emission. It has already been pointed out that the kpc-scale jet structure in NGC 6251 requires an ambient gas with temperatures of 2–5 keV to confine it. So far, the lack of detection of a gas component with such an high-temperature had led to the problem of an "over-pressurized" jet in NGC 6251. It would be tempting to speculate that the high-temperature thermal component measured by ASCA is the required "missing link" to ensure the thermodynamical stability of the kpc-scale jet. Unfortunately, only rather strict upper limits can be set on any X-ray emission associated with the radio jet (see Table 3). Alternatively, the line could be produced in the interaction between the "bloated" base of a jet with a stratified velocity structure and the circumnuclear matter, as proposed by Chiaberge et al. (2000) in the context of a possible unification model between BL Lac objects and FR I radio galaxies. The possibility that the iron line is associated with the highly ionized "skin" of an accretion disk cannot be in principle ruled out, although evidence for significantly ionized disk lines is rather scanty so far.

All the best-fit X-ray models discussed in this paper require an amount of cold photoelectric absorption in excess to the Galactic contribution. The weighted between the BeppoSAX and ASCA measurements is $N_{\rm H} = (1.06 \pm 0.11) \times 10^{21}$ cm^{-2}. This is in excellent agreement with the column density through the dusty disk, as derived from its visual extinction ($A_V = 0.61 \pm 0.12$; Ferrarese & Ford 1999), if standard gas-to-dust Galactic ratios are assumed. This is in agreement with the idea that the standard pc-scale optically and geometrically thick torus – even if present in FRI low-luminosity radio galaxies – does not intercept our line-of-sight to the nucleus (Chiaberge et al. 2002).

References

Arnaud, K., & Dorman, B. 2002, XSPEC User Manual v11.0
Arnaud, M., & Raymond, J. 1992, ApJ, 398, 394
Birkinshaw, M., & Worrall, D. M. 1993, ApJ, 412, 568
Boella, G., Butler, R. C., Perola, G. C., et al. 1997, A&AS, 122, 299
Boella, G., Chiappetti, L., Conti, G., et al. 1997, A&AS, 122, 327
Chiaberge, M., Capetti, A., & Celotti, A. 1999, A&A, 349, 77
Chiaberge, M., Celotti, A., Capetti, A., & Ghisellini, G. 2000, A&A, 358, 104
Chiaberge, M., Duccio Macchetto, F., Sparks, W. B., et al. 2002, ApJ, 571, 247
Chiaberge, M., Gilli, R., Capetti, A., Duccio & Macchetto, F. 2003, ApJ, in press [astro-ph/0307120]
Combi, J. A., Romero, C. E., Paredes, J. M., Torres, D. F., & Ribó, M. 2003, ApJ, 588, 731
Crane, P., & Vernet, J. 1997, ApJ, 486, L91
Di Matteo, T., Quataert, E., Allen, S. W., Narayan, R., & Fabian, A. C. 2000, MNRAS, 311, 507
Elvis, M., Wilkes, B. J., McDowell, J. C., et al. 1994, ApJS, 95, 1
Ferrarese, L., & Ford, H. C. 1999, ApJ, 515, 583
Fiore, F., Guainazzi, M., & Grandi, P. 1998, Cookbook of BeppoSAX data analysis (Roma: BeppoSAX SDC)
Fossati, G., Maraschi, L., Celotti, A., Comastri, A., & Ghisellini, G. 1998, MNRAS, 299, 433
Frontera, F., Costa, E., dal Fiume, D., et al. 1997, A&AS, 122, 347
Ghisellini, G., Haardt, F., & Matt, G. 1994, MNRAS, 267, 743
Guainazzi, M., Perola, G. C., Matt, G., et al. 1999, A&A, 346, 407
Ho, L. C. 1999, ApJ, 516, 672
Krolik, J. H., Madau, P., & Życki, P. T. 1994, ApJ, 420, L57
Jones, D. L., Unwin, S. C., Readhead, A. C. S., et al. 1986, ApJ, 305, 684
Liedahl, D. A., Osterheld, A. L., & Goldstein, W. H. 1985, ApJ, 438, L115
Mack, K. H., Kerp, J., & Klein, U. 1997, A&A, 324, 870
Marshall, H. L., Fruscione, A., & Carone, T. E. 1995, ApJ, 439, 90
Matsumoto, H., Koyama, K., Awaki, H., et al. 1997, ApJ, 482, 133
Matt, G., Fabian, A. C., & Ross, R. R. 1993, MNRAS, 261, 346
Matt, G., Brandt, W. N., & Fabian, A. C. 1996, MNRAS, 280, 823
Matt, G., Fabian, A. C., Guainazzi, M., et al. 2000, MNRAS, 318, 173
Matt, G., Guainazzi, M., Perola, G. C., et al. 2001, A&A, 377, L31
Mewe, R., Gronenschild, E. H. B. M., & van der Oord, G. H. J. 1985, A&AS, 62, 197

Mukherjee, R., Halpern, J., Mirabal, N., & Gotthelf, E. V. 2002, ApJ, 574, 693

Murphy, E. M., Lockman, F. J., Laor, A., & Elvis, M. 1996, ApJS, 105, 369

Narayan, R., & Yi, I. 1995, ApJ, 444, 231

Nieto, J. C., Coupinot, G., LeLievre, G., & Madsen, C. 1983, MNRAS, 203, 39P

Parmar, A. N., Martin, D. D. E., Bavdaz, M., et al. 1997, A&AS, 122, 309

Perley, R. A., Bridle, A. H., & Willis, A. G. 1984, ApJS, 54, 291

Prestage, R. M., & Peacock, J. A. 1988, MNRAS, 230, 131

Rees, M.J., Begelman, M. C., Blandford, R. D., & Phinney, E. S. 1982, Nature, 295, 17

Sambruna, R., Eracleous, M., & Mushotzky, R. 1999, ApJ, 526, 60

Sreekumar, P., Bertsch, D. L., Hartman, R. C., Nolan, P. L., & Thompson, D. J. 1999, Astropar. Physics, 11, 221

Sudou, H., Taniguchi, Y., Ohyama, Y., et al. 2001, PASJ, 52, 989

Tavecchio, F., Maraschi, L., & Ghisellini, G. 1998, ApJ, 509, 608

Turner, T. J., George, I. M., Nandra, K., & Mushotzky, R. F. 1997a, ApJS, 113, 23

Turner, T. J., George, I. M., Nandra, K., & Mushotzky, R. F. 1997b, ApJ, 488, 164

Wagget, P. C., Warner, P. J., & Baldwin, J. E. 1977, MNRAS, 181, 465

Werner, P. M., Worrall, D. M., & Birkinshaw, M. 2000, MNRAS, 317, 105

White, R. L., & Becker, R. H. 1992, ApJS, 79, 331

Young, P. J., Sargent, W. L. W., Kristian, J., & Westphal, J. A. 1979, ApJ, 234, 76